BIOCHEMISTRY
including biophysical chemistry & molecular biology

Article

pubs.acs.org/biochemistry

History-Dependent Depolymerization of Actin Filaments

Ishutesh Jain,[†] David Lacoste,[‡] Dulal Panda,[†] and Ranjith Padinhateeri*[,†]

[†]Department of Biosciences and Bioengineering, Indian Institute of Technology Bombay, Powai, Mumbai 400076, India
[‡]Laboratoire de Physico-Chimie Théorique, CNRS UMR Gulliver, ESPCI, 10 rue Vauquelin, Paris Cedex 05, France

Supporting Information

ABSTRACT: Depolymerizing cytoskeletal filaments are involved in cell division, cell motility, and other cellular functions. Understanding the dynamics of depolymerization is as important as understanding the dynamics of polymerization. We study nonequilibrium depolymerization of actin filaments using a simple two-state model. We show that the polymerization history influences the dynamics of depolymerization as well as the length fluctuations during depolymerization. We also simulate depolymerization under different experimentally feasible conditions. Under conditions of constant concentration, we show that the depolymerization happens in two regimes. Under the conditions of mass conservation, the depolymerization can have three regimes.

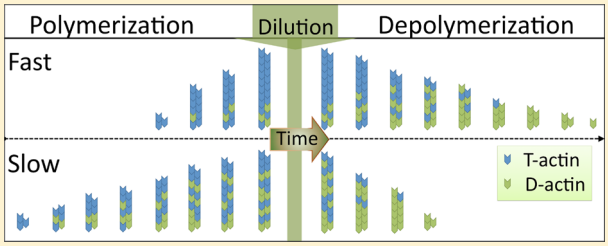

The cytoskeleton is a dynamic structure that maintains cell shape and allows many processes like cell motility and cell division.[1] Actin and microtubules are two of the well-known eukaryotic cytoskeletal filaments. Studies in the past decade have established that the cytoskeleton has a major role in prokaryotic cells also. FtsZ, ParM, etc., are some of the known cytoskeletal filaments in prokaryotes.[2−5] Even though all these filaments perform diverse set of functions, their polymerization dynamics have some common features. All these filaments polymerize and depolymerize by addition and removal of subunits at the end of the filaments. The binding of either ATP or GTP and the hydrolysis that occurs inside the filaments interfere with the polymerization dynamics in a complex way.[3,4,6]

Different groups have investigated the dynamics of single cytoskeletal filaments theoretically and experimentally. Research in the past three decades have provided a basic understanding of actin and microtubule polymerization.[3,7−15] The conventional understanding is that the dynamics of the cytoskeletal filaments is dictated by the chemical state of the polymerized subunits. If the subunits are ADP (GDP)-bound, they show a stronger tendency to depolymerize compared to the subunits bound to ATP (GTP).[3,8,11] The ATP (GTP) to ADP (GTP) conversion, known as ATP (GTP) hydrolysis, leads to many intriguing phenomena such as treadmilling and dynamic instability. Even though actin is not known to show dynamic instability, large length fluctuations have been reported for actin filaments.[16] Recently, a number of theoretical studies have provided quantitative predictions about the length fluctuations of biofilaments using models that couple the polymerization to ATP (GTP) hydrolysis in actin[17−20] or in microtubules.[21]

Typically, experiments with cytoskeletal filaments are concerned with the dynamics of polymerization and the filament properties at the steady state.[3,5,16,22] However, some recent experiments investigated the dynamics of depolymerization, under non-steady state conditions; some of them used dilution assays with single-filament resolution.[23,24] Kueh et al., investigating depolymerization dynamics of actin, found some intriguing behavior, which they thought was not following the conventional picture of actin polymerization kinetics. Cytoskeletal filaments having a ATP (GTP) cap are expected to depolymerize the cap first and then to depolymerize the ADP (GDP) part of the filament. This is expected to lead to a depolymerization dynamics having two regimes, slow depolymerization of the ATP (GTP) cap followed by fast depolymerization of the ADP (GDP) part. However, Kueh et al. found that actin depolymerization dynamics has sometimes three regimes with a second regime slower than the first, contrary to expectations.[23] They argued that this may be a result of plasticity in actin structures (whereby they mean the influence of the internal structure of the filament on its dynamics).[25] Interestingly, the experiments were conducted according to a protocol in which the actin filaments were polymerized for a very short time (1 min) and then depolymerization was observed after dilution. Jegou et al. performed a different kind of depolymerization experiment in which they depolymerized actin filaments in a flow experiment. Using a special flow setup, the concentration of the free subunits was fixed to a constant value throughout their experiment. They showed that their results, unlike those of Kueh et al., could be understood according to the conventional theory of actin kinetics.[24]

Such experiments with single filaments, with highly controlled microfluidics set up in particular, have the potential to precisely characterize dynamics of cytoskeletal filaments. To

Received: May 15, 2012
Revised: August 29, 2012
Published: August 30, 2012

   dx.doi.org/10.1021/bi300629f | *Biochemistry* 2012, 51, 7580−7587

understand the results of these experiments and to explore what can be obtained with such techniques, one requires a sound theoretical investigation that takes into account all the factors that are relevant to these experiments. Although many theoretical studies have investigated actin dynamics, none of them, to the best of our knowledge, systematically investigated depolymerization dynamics under conditions similar to those used in the experiments mentioned above. Most of the theoretical studies that investigate depolymerization dynamics of cytoskeletal filaments make certain assumptions about the polymerized filament. They usually assume that the polymerization, preceding depolymerization, leads to a steady state. Similarly, for the characterization of the dynamics of the filament, calculations are also generally performed in the long time limit assuming a steady state has been reached.[17−19] Much less is known about the dynamics of the filament length in non-steady state situations such as the ones corresponding to forced dilution, for instance. It is also not known how the history of the preparation of the filaments influences the filament dynamics at a later time.

In this paper, we present a computational study of depolymerization dynamics of actin filaments to answer these questions. We show that, depending on the conditions of the experiment, one can realize different types of depolymerization dynamics. We also show that the history of polymerization influences the depolymerization dynamics and length fluctuations and also perform a systematic study of the history-dependent dynamics. We also find that the length fluctuations are different in short filaments as compared to long ones.

MODEL

In this model, we consider an actin filament as a linear polymer of N subunits. Let d be the change in length of the filament when one subunit is added or removed.[18] Subunits can be added or removed at either end of the filament. The chemical state of ATP-bound subunits can be changed to the ADP-bound state via hydrolysis. Because of a set of differing views about questions related to hydrolysis, there are many models for the precise mechanism of hydrolysis. Some groups have argued that hydrolysis happens in a random manner, while others argue that it proceeds in a vectorial or cooperative fashion.[17−19,24,26−28] In this paper, we present simulations with the random mechanism of hydrolysis. Because conversion of ATP to ADP (ATP hydrolysis) is the crucial event that maintains the nonequilibrium nature of the cytoskeletal filaments, in this model we take into account only these two nucleotide states. In ref 28, a similar random model of hydrolysis with only two nucleotides was used, with the difference that this work assumes cooperative hydrolysis (i.e., hydrolysis that depends on the nucleotide state of neighboring units), which is not included in this work.

In this reduced description, we assume that each subunit exists in two states, either in the T state (ATP-bound state) or in the D state (ADP-bound state), and hydrolysis of the T subunit will lead to the D state. In the two-state model we use, there are seven kinetic events happening with different probabilities (see Figure 1). At the barbed end (denoted the + end), a T subunit can bind with a rate of U_T^+, and T and D subunits can dissociate, from the barbed end, with rates of W_T^+ and W_D^+, respectively. Similarly, at the pointed end (denoted the − end), a T subunit can add to the filament with a rate of U_T^-, and T and D subunits can be removed with rates of W_T^- and W_D^-, respectively. The association rates depend on the concentration of free T subunits such that $U_T^+ = k_0^+ C_T$ and $U_T^- = k_0^- C_T$, where k_0^+ and k_0^- are rate constants for the reactions and C_T is the free T subunit concentration. We assume that rate of D subunit polymerization is negligible compared to other rates. To model the hydrolysis, in the random mechanism, we assume that any T subunit, irrespective of its neighbor, can hydrolyze with a rate R_r. The various rate constant and rates associated with actin dynamics for this model are listed in Table 1.

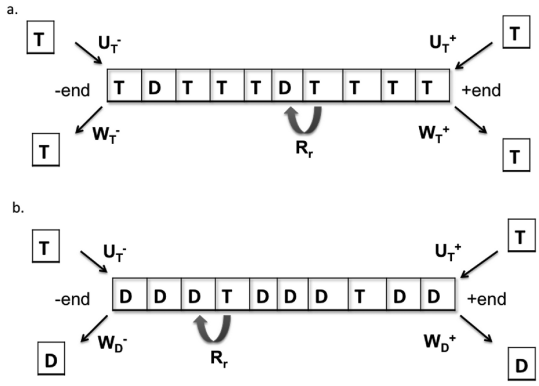

Figure 1. Schematic representation of various events that can occur during polymerization and depolymerization of a filament. (a) Events that are possible in the early stage of polymerization−depolymerization dynamics where filaments are mostly made of T-bound subunits. (b) Events associated with late stages of polymerization−depolymerization dynamics where most of the subunits in filaments are D-bound.

Table 1. Rate Constants and Rates Used in the Two-State Model

	k_0	W_T	W_D
+ end	11.6 μM^{-1} s^{-1}	1.4 s^{-1}	7.2 s^{-1}
− end	1.3 μM^{-1} s^{-1}	0.8 s^{-1}	0.27 s^{-1}

To mimic the depolymerization dynamics experiments, filaments are first polymerized at a high free subunit concentration for a time t_p and then depolymerized. This is performed under two different types of setups. In the first setup, we assume that the numbers of unbound (free) T subunits and D subunits remain unchanged. That is, the free subunit concentration of T-bound actin is C_T for all times. We call it the "constant concentration" setup (see Figure 2a). One may achieve this condition experimentally by appropriately allowing buffer and/or free subunits to flow in or out.[24]

In the second setup, we assume that the total number of subunits, during the whole of depolymerization, is conserved. That is, the sum of the number of subunits forming the filament, the number of free T subunits, and the number of free D subunits is always constant (see Figure 2b). Also, we assume that the free D subunits are not being converted back into T subunits, implying that at time $t \to \infty$ all actin subunits are D-bound. In the work, we call this setup the "mass conservation" setup. Once the dilution is performed, no material is added or removed from the system so that the mass is conserved. Typical dilution experiments, in which there is no replacement of buffer after dilution, will fall into this category.

Throughout this paper, we consider the dynamics of a single filament, assuming that there are no other filaments in the setup. Experimentally, this situation exists only in single-

dx.doi.org/10.1021/bi300629f | Biochemistry 2012, 51, 7580−7587

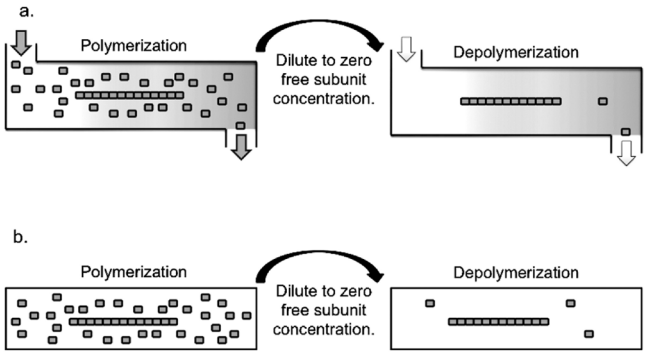

Figure 2. Schematic representation of different types of setups that we consider in our simulations. (a) Constant concentration setup. In this setup, the free subunit concentration is constant during both polymerization and depolymerization processes. Polymerization is conducted at a high free subunit concentration. Throughout the polymerization process, the concentration is kept constant (see the left part of panel a). Once the polymerization is complete, we suddenly dilute the system to zero free subunit concentration, triggering depolymerization. Depolymerization is occurring at a zero free subunit concentration. Throughout the depolymerization experiment, the concentration is kept to a constant value of zero (see the right part of panel a). This can be achieved by allowing free subunits to flow in and out. (b) Mass conservation setup. In this setup, during the polymerization−depolymerization process, the total numbers of subunits are conserved. Polymerization starts at a high free subunit concentration, and the concentration of free subunits decreases with polymerization. During this process of polymerization, we do not add or remove any material from the system. Once the polymerization is complete, we suddenly dilute the system to a zero free subunit concentration, triggering depolymerization. Once the depolymerization is started, we do not add or remove any material from the system. This means that, as the filament depolymerizes, the free subunit concentration will increase, keeping the total number of subunits after dilution conserved.

filament experiments, but we would expect the main results to be essentially similar if instead the experiment were to contain many filaments that are polymerized from fixed seeds. In this case, complete depolymerization of the filaments is avoided, and the number of filaments is kept constant. In the mass conservation setup, because no material is added or removed, the volume (V) of the system remains a constant. Because the number of filaments is constant, the concentration of the filaments defined as the number of filaments per unit volume ($C_f = 1/V$, when there is only a single filament in the volume) also remains constant.

We perform kinetic Monte Carlo simulations[19,29,30] and investigate the depolymerization dynamics of actin filaments under both setups mentioned above. Results from our simulations are discussed below.

RESULTS AND DISCUSSION

Depolymerization with a Constant Concentration. First, we present results of the depolymerization dynamics of actin filaments under the constant concentration condition. In these simulations, first, we polymerize the filament from a three-subunit seed, for a very short time (≈1 min), at a high monomer concentration such that the length reaches 5000 subunits. Then, to mimic dilution experiments, we set the free subunit concentration to zero and study the depolymerization dynamics. Because we enforce a constant free subunit concentration of zero, there is no polymerization during the course of this simulation. The result is shown in Figure 3. In this case, there are two clear regimes in the depolymerization

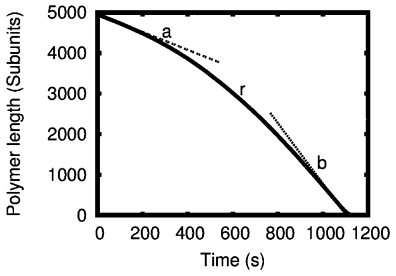

Figure 3. Depolymerization dynamics of the actin filament at a constant concentration. In this simulation, $R_r = 10^{-3}$ s^{-1}. Solid curve r shows the evolution of filament length during the course of the experiment. Line a has a slope of 2.2, and line b has a slope of 7.47.

dynamics, an early regime where depolymerization is slow compared to that in the later fast regime (also see Figure S3a of the Supporting Information for the velocity vs time curve). The first regime has a slope of 2.2 subunits/s, and the second regime has a slope of 7.47 subunits/s. These two regimes can be understood through the following simple argument. During the initial depolymerization regime, the filament mainly consists of ATP-bound subunits. Therefore, the change in average length (l) will obey

$$\frac{dl}{dt} = -(W_T^+ + W_T^-) \quad (1)$$

As shown in Table 1, $W_T^+ = 1.4$ s^{-1} and $W_T^- = 0.8$ s^{-1}, and this accounts for the slope of the first regime. When the time is much greater than the hydrolysis time ($t \gg 1/R_r$), nearly all subunits in the filament are hydrolyzed, and the change in length will be dominated by depolymerization of ADP-bound subunits such that

$$\frac{dl}{dt} = -(W_D^+ + W_D^-) \quad (2)$$

Because $W_D^+ = 7.2$ s^{-1} and $W_D^- = 0.27$ s^{-1}, we obtain the slope of the second regime, 7.47 s^{-1}. As mentioned in Model, this setup is similar to the experimental conditions in ref 24, and as expected, this result and data from ref 24 fit well for an R_r of 0.003 s^{-1} and a t_p of 10 min (see Figure S1 of the Supporting Information).

Depolymerization with Mass Conservation. Now we examine the depolymerization dynamics when there is mass conservation. As in the previous case, the filament was polymerized for a very short time (≈1 min), and then we set the free subunit concentration to zero, triggering depolymerization. For a fixed value of filament concentration (C_f = 0.33 nM), the result is shown in Figure 4. Unlike in the previous case, you can see three regimes here (also see Figure S3b of the Supporting Information for the velocity vs time curve). The first regime is dominated by the depolymerization of ATP-bound subunits. As the depolymerization of T subunits progresses, the free subunit concentration (C_T) increases, and therefore, the polymerization rate ($U_T^+ = k_0^+ C_T$) increases. This leads to a decrease in depolymerization velocity. Depending on the concentration of the filaments in the solution, after a certain time, the free subunit concentration in the solution reaches the critical concentration of the + end. At this point, the depolymerization happens mainly from the − end. This

dx.doi.org/10.1021/bi300629f | Biochemistry 2012, 51, 7580−7587

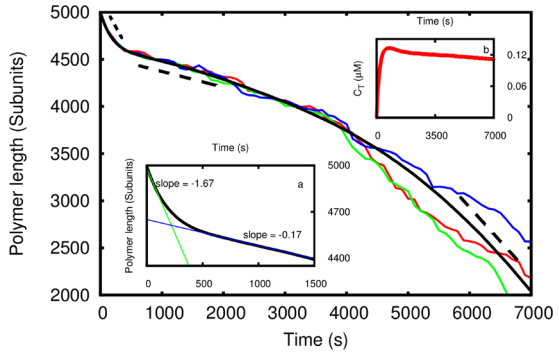

Figure 4. Depolymerization dynamics of actin filaments in the mass conservation setup. The solid black curve shows the change in average filament length with time (averaged over 100 simulations); various colored curves show depolymerization dynamics of individual filaments for a few representative filaments. In this simulation, $R_r = 10^{-3}$ s^{-1}. Here we can see three regimes. Dotted lines are given as a guide to the eye. Inset a is a magnification of the initial part of the solid black curve showing first two regimes. Inset b shows how C_T is changing during the simulation as depolymerizing T subunits are accumulating in solution.

essentially is the second regime in the graph. When the time $t \gg 1/R_r$, the ADP-bound subunit content is high, and this leads to a faster depolymerization. It is interesting to note that the slopes we obtain at different regimes are very close to the depolymerization velocities observed in the experiments of Kueh et al.[23] (see inset a). It should also be noted that the three regime dynamics are sensitive to filament concentration C_f (see Figure S4 of the Supporting Information).

To describe the events described above quantitatively, below we present a theoretical analysis of the depolymerization dynamics.

Theoretical Analysis of Depolymerization Dynamics. To improve our understanding of the depolymerization dynamics, we present a simple theoretical analysis here. We begin with writing a mean-field equation for the average length of the filament, taking into account all events, as

$$\frac{dl}{dt} = -W_T^+P_T^+ - W_T^-P_T^- - W_D^+(1 - P_T^+) - W_D^-(1 - P_T^-) + (k_0^+ + k_0^-)C_T \quad (3)$$

where P_T^+ is the probability of finding the T subunit at the + end and P_T^- is the probability of finding the T subunit at the − end. The first two terms represent the depolymerization of the T subunit from the + and − ends, respectively. Similarly, the third and fourth terms represent the depolymerization of the D subunit from either end. The last term indicates the polymerization happening at the + and − ends. Similar to the filament length, the free monomer concentration is also a time-dependent quantity obeying

$$\frac{1}{C_f}\frac{dC_T}{dt} = W_T^+P_T^+ + W_T^-P_T^- - (k_0^+ + k_0^-)C_T \quad (4)$$

The first two terms represent the increase in the free T subunit concentration caused by depolymerization, while the last term indicates the decrease in the T free subunit concentration caused by polymerization. Once we know $P_T^+(t)$ and $P_T^-(t)$, we can solve the coupled equations given above and obtain $l(t)$. $P_T^+(t)$ and $P_T^-(t)$, in general, will depend on addition, removal, and hydrolysis rates of the problem. In the steady state ($t \to \infty$), one can obtain an analytical expression for P_T^+.[19,21] However, obtaining time-dependent expressions for $P_T^+(t)$ and $P_T^-(t)$ is difficult. Therefore, below we make physically reasonable assumptions about $P_T^+(t)$ and $P_T^-(t)$ and solve the equations.

Because we polymerize the filament for a very short time ($t_p \ll 1/R_r$), at the beginning of the depolymerization, the filament mainly consists of T subunits; therefore, we assume that $P_T^+ = 1$. However, at later times, there is a non-zero probability that the − end subunits are hydrolyzed. For the sake of simplicity, we assume that, for a short period of time, P_T^- is a linear function of t; that is, $P_T^- = -\alpha^- t + \beta^-$, where α and β are two constants. On the basis of this assumption, we first solve eq 4 and obtain

$$C_T = \left[\frac{W_T^+}{k_0^+ + k_0^-} + \frac{W_T^-\beta^-}{k_0^+ + k_0^-} + \frac{W_T^-\alpha^-}{C_f(k_0^+ + k_0^-)^2}\right][1 - e^{-C_f(k_0^+ + k_0^-)t}] - \frac{W_T^-\alpha^- t}{k_0^+ + k_0^-} \quad (5)$$

Substituting this back in eq 3, we obtain

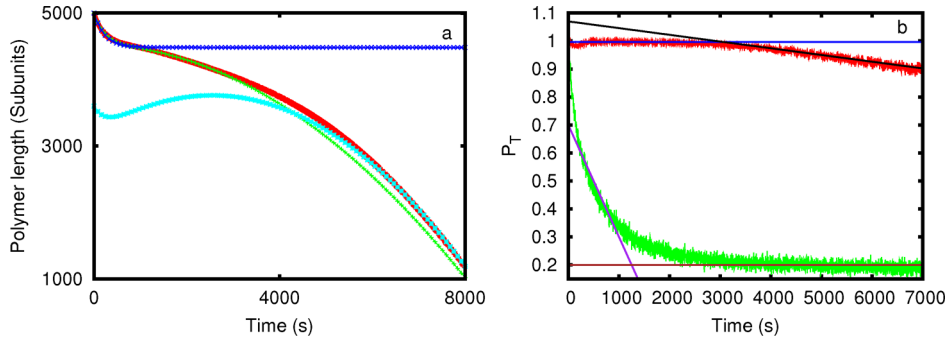

Figure 5. Theoretical analysis of depolymerization dynamics of actin under the mass conservation condition. (a) The red curve shows the evolution of average filament length with time as obtained from simulations. Equation 7 is plotted as the green curve here with an α^- of 0.0004 s^{-1} and a β^- of 0.7; this fits with the early regimes of the simulation data. The cyan curve shows eq 8 for $\alpha^+ = 0.000024$ s^{-1}, $\beta^+ = 1.09$, and $\beta^- = 0.2$ and fits with the late regime of the simulation data. The blue curve represents eq 8 for a hypothetical case where $P_T^+ = P_T^- = 1$. (b) Change in P_T^+ (red) and P_T^- (green) as a function of time during the course of depolymerization obtained from the simulation. The other curves represent the following: $P_T^+ = 1$ (blue), $P_T^- = -0.0004t + 0.7$ (purple), $P_T^+ = -0.000024t + 1.09$ (black), and $P_T^- = 0.2$ (brown).

dx.doi.org/10.1021/bi300629f | Biochemistry 2012, 51, 7580−7587

$$\frac{dl}{dt} = \frac{W_T^- \alpha^-}{C_f(k_0^+ + k_0^-)} - W_D^-(1 + \alpha^- t - \beta^-) - \left[W_T^+ + W_T^- \beta^- + \frac{W_T^- \alpha^-}{C_f(k_0^+ + k_0^-)}\right] e^{-C_f(k_0^+ + k_0^-)t} \quad (6)$$

Solving equation 6, we obtain the average length as a function of time

$$l = l_o + \frac{W_T^- \alpha^- t}{C_f(k_0^+ + k_0^-)} - W_D^-\left(t + \frac{\alpha^- t^2}{2} - \beta^- t\right) - \left[W_T^+ + W_T^- \beta^- + \frac{W_T^- \alpha^-}{C_f(k_0^+ + k_0^-)}\right] \frac{1 - e^{-C_f(k_0^+ + k_0^-)t}}{C_f(k_0^+ + k_0^-)} \quad (7)$$

where l_o is the initial filament length. We fit the early time simulation data to eq 7 and find that $\alpha^- = 0.0004\ s^{-1}$ and $\beta^- = 0.7$ (Figure 5, green curve). This has an interesting implication: analyzing the depolymerization dynamics data, our simple theory can make predictions about the nature of cap dynamics. Our theory predicts the behavior of P_T^- at the early time of the depolymerization. To test our prediction, we compute P_T^+ and P_T^- from our simulation, and the result is shown in Figure 5b. We find that, during the early period of depolymerization, $P_T^+ = 1$ and the dominating behavior of P_T^- is very close to what we predicted ($P_T^+ = -0.0004t + 0.7$). We also compared this theoretical formula (eq 7) to experimental data from ref 23. As seen in the Supporting Information (Figure S2), our equation fits well with the data for $P_T^- = -0.0002t + 1$ and $C_f = 0.00026\ \mu M$.

When $t \gg 1/R_r$, P_T^+ starts to deviate from 1. Therefore, to understand the dynamics of the filament for $t \gg 1/R_r$, on the basis of our simulation data of P_T^+ and P_T^- (Figure 5b), we assume that $P_T^+ = -\alpha^+ t + \beta^+$ and $P_T^- = \beta^+$, a constant. With these assumptions, we solve eqs 3 and 4 and obtain

$$l = l_o + \frac{C_o}{C_f}[e^{-C_f(k_0^+ + k_0^-)t} - 1] + \frac{W_T^+ \alpha^+}{C_f(k_0^+ + k_0^-)} t - W_D^+\left(t + \frac{\alpha^+ t^2}{2} - \beta^+ t\right) - W_D^-(t - \beta^- t) + \left[W_T^+ \beta^+ + W_T^- \beta^- + \frac{W_T^+ \alpha^+}{C_f(k_0^+ + k_0^-)}\right] \frac{e^{-C_f(k_0^+ + k_0^-)t} - 1}{C_f(k_0^+ + k_0^-)} \quad (8)$$

On the basis of our simulation results shown in Figure 5b, we take $\alpha^+ = 0.000024\ s^{-1}$, $\beta^+ = 1.09$, and $\beta^- = 0.2$. Using these values, we plot eq 8 (Figure 5a, cyan curve) and find that the curve fits very well with the simulation data (Figure 5a, red curve). This shows that once we know the dynamics of P_T^+ and P_T^-, we can obtain the filament dynamics using a simple analytical theory.

In Figure 5a, we also show our analytical result when $P_T^+ = P_T^- = 1$ for all times (blue curve). This is a case in which there is no hydrolysis. Note that the initial regime is comparable to the case with hydrolysis. This suggests that hydrolysis has no big role in deciding the dynamics in this regime. Also note that there is no third regime here, suggesting that hydrolysis plays an important role in deciding the dynamics in the third regime.

History Dependence of Depolymerization. Because the depolymerization dynamics after dilution is a nonequilibrium process, it is likely that it will depend on the history of the filament. Here we investigate how the history of polymerization affects the depolymerization dynamics. Below we present three different cases: (a) polymerization and depolymerization of filaments at a constant concentration, (b) polymerization with mass conservation and depolymerization at a constant concentration, and (c) polymerization and depolymerization with mass conservation. In each case, we polymerize the filament in two different ways: (i) for a short time such that the polymerization time $t_p \ll 1/R_r$ and (ii) for a long time such that $t_p \gg 1/R_r$.

Polymerization and Depolymerization at a Constant Concentration. First, we polymerize the filament for 1 min at a constant concentration of ≈8 μM such that it polymerizes to a length of 5000 subunits in the given time. Then we set the free subunit concentration to zero, such that the depolymerization is observed. The result is curve g in Figure 6a. Because polymerization time $t_p \ll 1/R_r$, most of the filament consists of

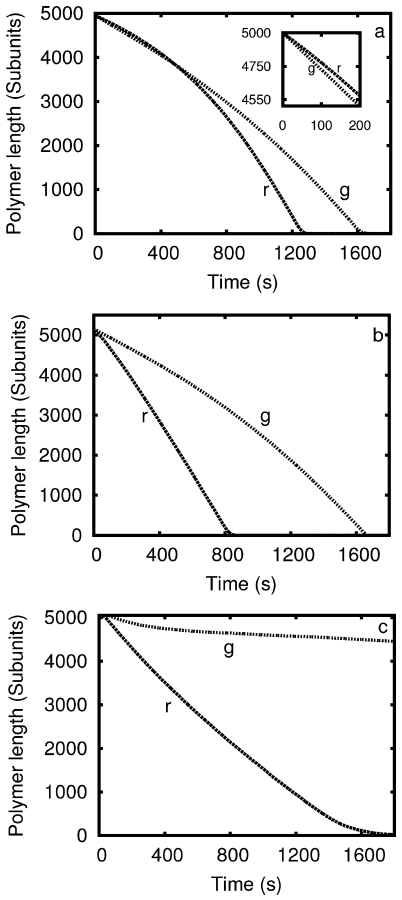

Figure 6. Dependence of depolymerization dynamics on the history of polymerization. The depolymerization dynamics for different cases are shown. In each panel, curves marked with a g represent data for the filaments that are polymerized for a very short time ($t_p \ll 1/R_r$). Curves marked with an r represent data for the filaments that are polymerized for a long time ($t_p \gg 1/R_r$). In all the cases here, $R_r = 10^{-3}\ s^{-1}$. (a) Polymerization and depolymerization under the constant concentration condition. (b) Polymerization under the mass conservation condition and depolymerization under the constant concentration condition. (c) Both polymerization and depolymerization under the mass conservation condition.

dx.doi.org/10.1021/bi300629f | Biochemistry 2012, 51, 7580−7587

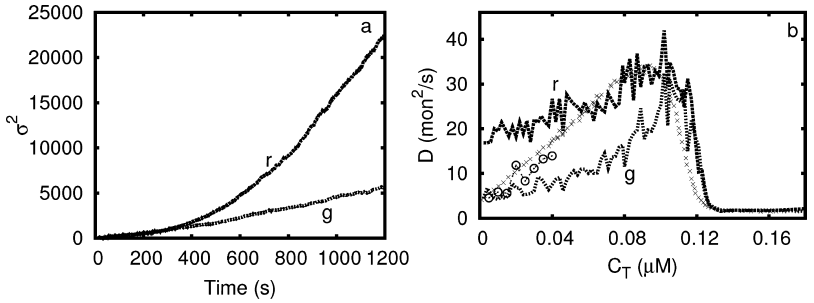

Figure 7. History dependence in length fluctuations. (a) σ^2 vs time plot for depolymerization dynamics and its relationship with history. Curve g stands for $t_p \approx 1$ min and curve *r* for $t_p \approx 50$ min. (b) Plot of diffusion coefficients at different concentrations. To obtain points below the critical concentration, filaments are polymerized for a time t_p to reach a length of 5000 subunits; then filaments are depolymerized by reducing the concentration to a fixed value indicated by C_T, and diffusion coefficients are calculated during the course of depolymerization. Curve g and curve r stand for case 1 ($t_p \ll 1/R_r \approx 1$ min) and case 2 ($t_p \gg 1/R_r \approx 50$ min), respectively. Times signs represent diffusion coefficients as calculated previously.[17,29] Empty circles represent diffusion coefficients calculated during depolymerization of long filaments (length of 20000 subunits).

T subunits and the depolymerization dynamics in the early time is dictated by eq 1. However, as time progresses, T subunits start to hydrolyze and the depolymerization obeys the following equation.

$$\frac{dl}{dt} = -W_T^+ P_T^+ - W_T^- P_T^- - W_D^+(1 - P_T^+) - W_D^-(1 - P_T^-) \tag{9}$$

As the equation suggests, here, the depolymerization dynamics is a combination of T depolymerization and D depolymerization. For appropriate values of P_T^+, one can obtain the velocity seen in this regime of curve g. It can be seen that whenever $P_T^{\pm} < 1$, the depolymerization velocity from eq 9 is going to be larger than that from eq 1. Therefore, the slope of the late time regime, in curve g, will be greater than that of the early time regime.

Second, we polymerize the filament for a long time ($t_p \gg 1/R_r$) at a constant concentration of 0.3 μM such that the filament reaches the same length as the previous case (5000 subunits) in ≈45 min. Then we depolymerize the filament at a zero subunit concentration and the result is curve r in Figure 6a. The long polymerization results in a filament with a large D content with nearly no T subunits at the − end. Therefore, the first regime in the depolymerization dynamics is a regime in which ATP subunits are depolymerized from the + end and ADP subunits are depolymerized from the − end such that

$$\frac{dl}{dt} = -(W_T^+ + W_D^-) \tag{10}$$

Note that this is different from the previous case (curve g), given by eq 1, and the difference is highlighted in the inset. The polymerization at a low concentration results in a small T cap[21,29] at the + end. This implies that the first regime is relatively shorter than curve g. As time progresses, the D content increases further, and the depolymerization seen in the second regime is faster. Even though the dynamics is given by eq 9, because the D content of the filament is much greater (see Figure S5 of the Supporting Information), the dominating term is $-W_D(1 - P_T)$. Therefore, compared to curve g, the second regime here is much faster.

Polymerization with Mass Conservation and Depolymerization at a Constant Concentration. In this simulation, first, we polymerize the filament, under the mass conservation condition, for 1 min ($t_p \ll 1/R_r$), such that the total length is ≈5000 subunits at the given time. Then we observe the depolymerization at a zero subunit concentration for all times, and the result is shown in Figure 6b (curve g). On the short time scale of polymerization, the mass conservation condition does not influence the content of the filament much. Therefore, the dynamics in this case is exactly the same as curve g in Figure 6a.

In the second simulation, we polymerized the filament, under mass conservation, for a period of 50 min ($t_p \gg 1/R_r$) to reach the final length of ≈5000 subunits. Then depolymerization was initiated fixing a constant subunit concentration of zero. The result is shown in Figure 6b (curve r). Comparing curve r of this simulation with curve r of the previous case (Figure 6a), we find that the depolymerization dynamics is completely different. When polymerization was conducted at a constant concentration, the depolymerization dynamics showed two regimes; however, here, the depolymerization dynamics has only one regime, the faster depolymerizing regime. To understand this further, we computed the dynamics of the T content of the filament for both cases. We find that polymerization under mass conservation leads to a much smaller T content compared to the case of polymerization at a constant concentration (see Figure S5 of the Supporting Information). The large D content in this case leads to a faster depolymerization with a velocity dominated by the $-W_D(1 - P_T)$ term in eq 9.

Polymerization and Depolymerization with Mass Conservation. Here, unlike the previous cases, we perform polymerization and depolymerization simulations with mass conservation. The polymerization dynamics is exactly the same as in the previous case. First, we polymerize the filament under the mass conservation condition, for 1 min. Then the depolymerization simulation is performed with mass conservation. The result is plotted as curve g in Figure 6c. The dynamics is similar to that of the curves shown in Figure 4a.

In the second simulation, using the similar polymerization dynamics as in the previous case, we polymerize the filament for 50 min to reach the final length of ≈5000 subunits, and then by setting the free subunit concentration to zero, we observe depolymerization under the mass conservation condition. The resultant dynamics is shown in Figure 6c as curve r. The key difference between this dynamics and curve r in Figure 6b is that here, at later times, the addition of subunits will also play an important role. As expected, in the early period, the depolymerization velocity is comparable to that of curve r in Figure 6b; however, as time progresses, the free subunit concentration increases and the contribution of the $k_0 C_T$ term

dx.doi.org/10.1021/bi300629f | *Biochemistry* 2012, 51, 7580−7587

in eq 3 starts to decrease the velocity. Therefore, we obtain a slower depolymerization compared to the previous case.

In each of the three cases presented above, the depolymerization condition, for a given case, is exactly the same for curves g and curves r. Still, there is a major difference in the depolymerization dynamics. The reason for this difference is that the history of polymerization does affect the depolymerization dynamics. That is, the depolymerizing filaments have a memory of their polymerization history.

History Dependence in Length Fluctuations. In this section, we study the length fluctuations of the depolymerizing filaments and investigate how the history of the filament polymerization influences these fluctuations. Length fluctuations can be quantified by defining variance as

$$\sigma^2(t) = \langle l(t)^2 \rangle - \langle l(t) \rangle^2 \tag{11}$$

In Figure 7a, we have plotted σ^2 as a function of time for two cases: (1) when the filament is polymerized for a short time ($t_p \ll 1/R_r$) and depolymerized at a constant concentration of 0.02 μM (curve g) and (2) when the filament is polymerized for a long time ($t_p \gg 1/R_r$) and depolymerized at a constant concentration of 0.02 μM (curve r). Here we have two cases with different histories of polymerization, and in both the cases, we calculate $\sigma^2(t)$ when the filament is depolymerizing. As you can see from the figure, the history of polymerization does affect the length fluctuations. In both the cases, at later times, one can see that σ^2 increases linearly with time as observed, for instance, experimentally in ref 16. In analogy with the definition of the diffusion coefficient used to characterize Brownian motion, one can define for this case a diffusion coefficient as[16,17,19,31]

$$D = \lim_{t\to\infty} \frac{1}{2} \frac{d\sigma^2(t)}{dt} \tag{12}$$

Here, we calculate the derivative at the longest time possible, just before the filament completely depolymerizes to a zero length. At this point in time, as seen Figure 7a, $\sigma^2(t)$ is a linear function of t. Using eq 12, we compute the diffusion coefficient for different concentrations for both cases discussed above. The result is shown in Figure 7b. Curve g corresponds to case 1 ($t_p \approx 1$ min $\ll 1/R_r$), and curve r corresponds to case 2 ($t_p \approx 50$ min $\gg 1/R_r$). The results indicate that the diffusion coefficient, below the critical concentration (C_c), does depend on the history of polymerization. Below C_c, the diffusion coefficient for case 1 is small compared to the diffusion coefficient for case 2. It has been shown that the diffusion coefficient when there are only T subunits in a filament will be smaller than when there are T and D monomers in the filament.[17,19,31] In our case 1, because we polymerized the filament for only a very short time, as we have discussed in the previous sections, the T content of the filament will be much greater than the D content. However, in case 2, the D content of the filament will be larger. This explains why the diffusion coefficient of case 1 is smaller than that of case 2.

We compared our results for the diffusion coefficient with the results reported previously[17,29] (data points are shown as times signs (×)) and found that, in the depolymerizing regime (where $C_T < C_c$), our results are very different. It turns out that the observed difference stems from an important assumption made in the previous works. While computing diffusion coefficients, the earlier works assume that depolymerizing filaments are very long such that the diffusion coefficient can be computed in the $t \to \infty$ limit. However, in our case, the filaments are finite. We restrict the maximal size of the filament to 5000 subunits as it is unrealistic to have very long filaments in experiments.[15] This explains how our results are different from earlier results. To test whether the difference is indeed because of the finite size filaments we take, we investigate depolymerization of long filaments (20000 subunits) and compute the diffusion coefficient during depolymerization of long filaments. This results in diffusion coefficients that are comparable to those of the earlier works (see the empty circles; also see Figure S6 of the Supporting Information). This suggests that, when experimentally measuring the length fluctuations, the finite size effect and the history of polymerization of the filament are both important in determining the amount of fluctuations.

Suggestions for New Experiments for Testing Our Predictions. Our theoretical studies show that the depolyrization dynamics depends on the history of polymerization. In this work, we provide a number of predictions about how various parameters, like polymerization time (t_p), the concentration of filaments (C_f), and the precise conditions such as mass conservation or constant concentration, affect the length dynamics and length fluctuations. This can be tested experimentally.

First, to test whether the three-regime dynamics is a consequence of the optimal filament concentration under the mass conservation condition, we suggest an experiment in a mass conservation setup that can check the effect of filament concentration (C_f) on the depolymerization dynamics, keeping the polymerization time (t_p) constant. This may be achieved by setting up experiments in which polymerization and depolymerization happen starting from a set of seeds (nucleation sites) and precisely controlling the concentration of these seeds.

Second, we propose an experiment in which one can carefully quantify the effect of polymerization time (t_p) on the depolymerization dynamics under the mass conservation condition and the constant concentration condition. Such experiments can also test whether the length fluctuations depend on the history of polymerization, as we predict in our paper. As we mentioned earlier, the constant concentration setup may be achieved via controlled microfluidic setups.

CONCLUSION

In this paper, we have analyzed the depolymerization dynamics of actin filaments under different experimentally feasible conditions. We have investigated how these different conditions influence the depolymerization dynamics and how the history of polymerization affects the depolymerization dynamics. We find that the depolymerizing filaments do have a memory of their polymerization history. The length fluctuations of the filament, which we quantify using a diffusion constant, are also determined by the history of polymerization. We have also shown that, depending on the experimental conditions, one can expect depolymerization dynamics with two or three regimes. While our paper shows what one can expect from a conventional model of actin kinetics, it is possible that some effects that are not discussed here may lead to intriguing actin dynamics. For example, a recent paper has claimed that the slowing down of depolymerization of the actin filament seen in the work of Kueh et al. is due to photoinduced dimerization of actin subunits.[32]

In the simple two-state model presented here, in which subunits are either ATP-bound or ADP-bound, the hydrolysis

time scale plays an important role in the history-dependent depolymerization. Filaments that are polymerized for a very short time behave differently compared with filaments that are polymerized for a long time. This might have important ramifications for the dynamics of cytoskeletal filaments in vivo. These results could be extended to other biological filaments like microtubules and FtsZ that share many similar features with actin.

As far as the modeling of hydrolysis is concerned, one could also develop a more complex model with more than just two conformational states or including cooperativity in the form of a dependence of hydrolysis on the state of nearby subunits. One limitation of our model is that we assume that cytoskeletal filaments behave as linear polymers obeying simple chemical kinetics laws. However, to understand the depolymerization dynamics and the resulting force generation in filaments like microtubules, one might need to invoke a more complex mechanochemical model that couples the chemical kinetics with the filament structure and with its mechanical properties.

■ ASSOCIATED CONTENT

Supporting Information

Comparison with experimental data and extra material that supplements the data in the paper. This material is available free of charge via the Internet at http://pubs.acs.org.

■ AUTHOR INFORMATION

Corresponding Author

*Department of Biosciences and Bioengineering, Indian Institute of Technology Bombay, Powai, Mumbai 400076, India. Phone: +91 22 25767761. E-mail: ranjithp@iitb.ac.in.

Funding

R.P. acknowledges funding from the Department of Biotechnology India through IYBA. D.P. is thankful for a DAE SRC fellowship from the Government of India. I.J. acknowledges a fellowship from CSIR, India. D.L. acknowledges funding from Agence Nationale pour la Recherche (ANR).

Notes

The authors declare no competing financial interest.

■ REFERENCES

(1) Alberts, B., Johnson, A., Lewis, J., Raff, M., Roberts, K., and Walter, P. (2002) *Molecular Biology of the Cell*, 4th ed., Garland Science, New York.

(2) Graumann, P. L. (2007) Cytoskeletal elements in bacteria. *Annu. Rev. Microbiol. 61*, 589−618.

(3) Carlier, M.-F. (1990) Actin polymerization and ATP hydrolysis. *Adv. Biophys. 26*, 51−73.

(4) Howard, J. (2001) *Mechanics of Motor Proteins & the Cytoskeleton*, Sinauer Associates, Sunderland, MA.

(5) Pollard, T. D., and Borisy, G. G. (2003) Cellular motility driven by assembly and disassembly of actin filaments. *Cell 112*, 453−465.

(6) Phillips, R. B., Kondev, J., and Theriot, J. (2009) *Physical Biology of the Cell*, Garland Science, New York.

(7) Korn, E. D., Carlier, M.-F., and Pantaloni, D. (1987) Actin polymerization and ATP hydrolysis. *Science 238*, 638−644.

(8) Pollard, T. D. (1986) Rate constants for the reactions of ATP- and ADP-actin with the ends of actin filaments. *J. Cell Biol. 103*, 2747−2754.

(9) Pantaloni, D., Hill, T. L., Carlier, M.-f., and Korn, E. D. (1985) A model for actin polymerization and the kinetic effects of ATP hydrolysis. *Proc. Natl. Acad. Sci. U.S.A. 82*, 7207−7211.

(10) Mitchison, T., and Kirschner, M. (1984) Dynamic instability of microtubule growth. *Nature 312*, 237−242.

(11) Desai, A., and Mitchison, T. J. (1997) Microtubule polymerization dynamics. *Annu. Rev. Cell Dev. Biol. 13*, 83−117.

(12) Wegner, A. (1976) Head to tail polymerization of actin. *J. Mol. Biol. 108*, 139−150.

(13) Panda, D., Miller, H. P., and Wilson, L. (1999) Rapid treadmilling of brain microtubules free of microtubule-associated proteins in vitro and its suppression by tau. *Proc. Natl. Acad. Sci. U.S.A. 96*, 12459−12464.

(14) Margolis, R. L., and Wilson, L. (1981) Microtubule treadmills: Possible molecular machinery. *Nature 293*, 705−711.

(15) Sept, D., Xu, J., Pollard, T. D., and Mccammon, J. A. (1999) Annealing accounts for the length of actin filaments formed by spontaneous polymerization. *Biophys. J. 77*, 2911−2919.

(16) Fujiwara, I., Takahashi, S., Tadakuma, H., Funatsu, T., and Ishiwata, S. (2002) Microscopic analysis of polymerization dynamics with individual actin filaments. *Nat. Cell Biol. 4*, 666−673.

(17) Vavylonis, D., Yang, Q., and O'Shaughnessy, B. (2005) Actin polymerization kinetics, cap structure, and fluctuations. *Proc. Natl. Acad. Sci. U.S.A. 102*, 8543−8548.

(18) Stukalin, E. B., and Kolomeisky, A. B. (2006) ATP hydrolysis stimulates large length fluctuations in single actin filaments. *Biophys. J. 90*, 2673−2685.

(19) Ranjith, P., Lacoste, D., Mallick, K., and Joanny, J.-F. (2009) Nonequilibrium self-assembly of a filament coupled to ATP/GTP hydrolysis. *Biophys. J. 96*, 2146−2159.

(20) Carlsson, A. E. (2006) Stimulation of actin polymerization by filament severing. *Biophys. J. 90*, 413−422.

(21) Padinhateeri, R., Kolomeisky, A. B., and Lacoste, D. (2012) Random Hydrolysis Controls the Dynamic Instability of Microtubules. *Biophys. J. 102*, 1274−1283.

(22) Carlier, M.-f., Pantaloni, D., and Korn, E. D. (1986) The effects of Mg^{2+} at the high-affinity and low-affinity sites on the polymerization of actin and associated ATP hydrolysis. *J. Biol. Chem. 261*, 10785−10792.

(23) Kueh, H. Y., Brieher, W. M., and Mitchison, T. J. (2008) Dynamic stabilization of actin filaments. *Proc. Natl. Acad. Sci. U.S.A. 105*, 16531−16536.

(24) Jégou, A., Niedermayer, T., Orbán, J., Didry, D., Lipowsky, R., Carlier, M.-F., and RometLemonne, G. (2011) Individual Actin Filaments in a Microfluidic Flow Reveal the Mechanism of ATP Hydrolysis and Give Insight Into the Properties of Profilin. *PLoS Biol. 9*, e1001161.

(25) Kueh, H. Y., and Mitchison, T. J. (2009) Structural plasticity in actin and tubulin polymer dynamics. *Science 325*, 960−963.

(26) Ohm, T. (1994) Mechanism of ATP hydrolysis by polymeric actin. *Biochim. Biophys. Acta 1208*, 8−14.

(27) Carlier, M.-F., Pantaloni, D., and Korn, E. D. (1987) The Mechanisms of ATP Hydrolysis Accompanying the Polymerization. *J. Biol. Chem. 262*, 3052−3059.

(28) Li, X., Lipowsky, R., and Kierfeld, J. (2010) Coupling of actin hydrolysis and polymerization: Reduced description with two nucleotide states. *Europhys. Lett. 89*, 38010.

(29) Ranjith, P., Mallick, K., Joanny, J.-F., and Lacoste, D. (2010) Role of ATP-hydrolysis in the dynamics of a single actin filament. *Biophys. J. 98*, 1418−1427.

(30) Gillespie, D. T. (1977) Exact stochastic simulation of coupled chemical reactions. *J. Phys. Chem. 81*, 2340−2361.

(31) Stukalin, E. B., and Kolomeisky, A. B. (2005) Polymerization dynamics of double-stranded biopolymers: Chemical kinetic approach. *J. Chem. Phys. 122*, 104903.

(32) Niedermayer, T., Jégou, A., Chièze, L., Guichard, B., Helfer, E., Romet-Lemonne, G., Carlier, M.-F., and Lipowsky, R. (2012) Intermittent depolymerization of actin filaments is caused by photo-induced dimerization of actin protomers. *Proc. Natl. Acad. Sci. U.S.A. 109*, 10769−10774.